

SEISMIC RESPONSE OF TWO BUILDING STRUCTURES DESIGNED FOR HIGH SEISMIC HAZARD

C.A. Arteta & H.R. Esquivel

Universidad del Norte, Colombia

J.P. Moehle

University of California at Berkeley, USA

H. Carlosama

Universidad Pedagógica y Tecnológica de Colombia, Colombia



SUMMARY

The performance of code-compliant structural designs under realistic scenarios of seismic hazard is still being tested. Two reinforced concrete structures of 4 and 12 stories, designed under the provisions of current building codes (e.g. NSR-10, ASCE-7 and ACI-318) and located on a high seismicity hazard site, are studied in this paper. By means of nonlinear dynamic analyses, this study assesses the adequacy of code-compliant earthquake-resistant-designs for structures undergoing different sources of seismic demand: specifically, i) shallow crustal earthquakes, ii) deep subduction earthquakes and iii) shallow subduction earthquakes. The results of the case study provide a comparison between the expected performance of code-compliant structures and actual performance as represented by numerical models. The case study suggests that the estimations of seismic demand proposed by actual building codes do not necessarily lead to adequate estimations of realistic demands on key components of the structures.

Keywords: nonlinear analyses, seismic assessment, code-compliant, subduction, crustal.

1. INTRODUCTION

The west portion of South America is part of the circum-Pacific seismic belt where high seismic hazard is an integral part of the daily life in countries such as Colombia, Ecuador, Perú and Chile. In this part of the world, the complex interaction between the Nazca plate and the Suramerican plate in a subduction boundary has given birth to a series of faults that constitute seismic hazard sources for cities located along the coast of the Pacific Ocean.

This case study focuses on the structural response of two reinforced concrete buildings assumed to be located in Santiago de Cali, Colombia. This city is of particular interest, because its seismic hazard is related to three different earthquake sources: i) shallow crustal sources, ii) a deep subduction source and iii) a shallow subduction source (INGEOMINAS, 2005). In addition, the city is located on a sedimentary deposit of layered clayey and sandy materials, which overlay the base rock. These circumstances, which are very common in many cities in Colombia and urbanized areas around the world, make the dynamic behaviour of the soils very complex and introduce site effects that need to be considered. Site response analysis using SHAKE 2000 (Ordoñez, 2000) were performed to define the ground motions demands at the ground surface.

The buildings were designed to comply with the local building code (NSR-10, 2010) and well-known codes used around the world such as ASCE-7, 2006 and ACI-318, 2011. The adequacy of code-compliant earthquake-resistant-designs for structures undergoing strong shaking is discussed. The realistic seismic hazard scenario selected for this study is made up of 40 ground motions consistent with the seismic hazard scenarios described above. Results of structural responses from numerical nonlinear modelling of the

buildings are presented.

The results of the case study provide a comparison between the expected performance of a code-compliant structure and actual performance as represented by numerical models. The case study suggests that the estimations of seismic demand proposed by actual building codes do not necessarily lead to adequate estimations of realistic demands on key components of the structures. The results suggest the high potential for relatively brittle failures in some key components for levels of shaking that are smaller than the design level.

2. ESTIMATION OF THE SEISMIC DEMAND

The buildings under consideration were assumed to be located on a site that coincides with the location of the Colombian Geological Survey Office (INGEOMINAS) in Santiago de Cali Colombia (Long.: - 76.5396, Lat.: 3.3727). This site was selected because geotechnical properties of the soil profile has been well characterized (INGEOMINAS, 2005), and also because this site is instrumented with an accelerometer station that has recorded past ground motions that make feasible the calibration of the soil model for site response analysis.

The selected site corresponds geologically to the *Meléndez and Lily Aluvian fan*. The soil profile is composed of a 9 m layer of silty soil overlying granular layers of silty and clayey sands, gravels and blocks of rocks that are intercalated with thin layers of fine soils, predominantly clays. The depth to the alluvial plain is about 50 m and to the base rock has been estimated at about 130 m. The shear wave velocity of the silty layer varies between 200 and 300 m/s while non-cohesive soils showshear wave velocities between 300 m/s and 700 m/s. The shear wave velocity over the top 30 meters (V_{s30}) for this site was estimated as 270 m/s. A very detailed description of the soil profile and its geotechnical properties can be found in INGEOMINAS, 2005.

The seismic demand estimation for this case study follows closely the recommendations contained in the microzonation study entitled “*Estudio de Microzonificación Sísmica de Santiago de Cali*” (INGEOMINAS, 2005). This study defines the seismic hazard scenarios for different zones within Santiago de Cali according to the general tectonic and geological environment surrounding the city as well as site specific characteristics of the underlying soil of the zones. The three hazard scenarios considered are due to: i) *crustal shallow earthquakes*, ii) *deep subduction earthquakes* and iii) *shallow subduction earthquakes*. In total 20 pairs of ground motions were selected to represent the seismic hazard for outcropping rock at the site: 12 for the crustal scenario (12CEQ), 16 for deep subduction earthquakes (16DEQ) and 12 for the shallow subduction earthquakes (12SEQ). Selection was done following the criteria described on Table 1. Both horizontal components of each recording were included in the analysis.

Table 1. Ground motions selection criteria

Scenario	Focal Depth [km]	Moment Magnitude [Mw]	Epicentral Distance [km]	Horizontal PGA [g]
Crustal (12C)	0 to 30	5.8 to 6.5	20 to 100	0.17 to 0.23
Deep Subduction (16D)	70 to 200	6.8 to 7.8	20 to 200	0.17 to 0.23
Shallow Subduction (12S)	10 to 40	7.5 to 9.0	70 to 300	0.10 to 0.23

The site response analyses were performed using a 1D-equivalent-linear approach incorporated in SHAKE 2000 (Ordoñez, 2000). A simplified soil profile model was implemented and calibrated based on the actual geotechnical and geometrical properties of the soil column and on a previous recorded ground motion. The selected outcropping rock motions were brought and converted to equivalent rock motions at the base of the soil profile and then, they were run through the soil profile to get the outcropping soil motions, which were finally considered in the structural nonlinear dynamic analyses. The corresponding

spectra of those outcropping soil motions are presented in Figure 1. Figure 1d also shows the elastic design response spectrum used as the seismic demand for the code-compliant analysis and design of the buildings (INGEOMINAS, 2005).

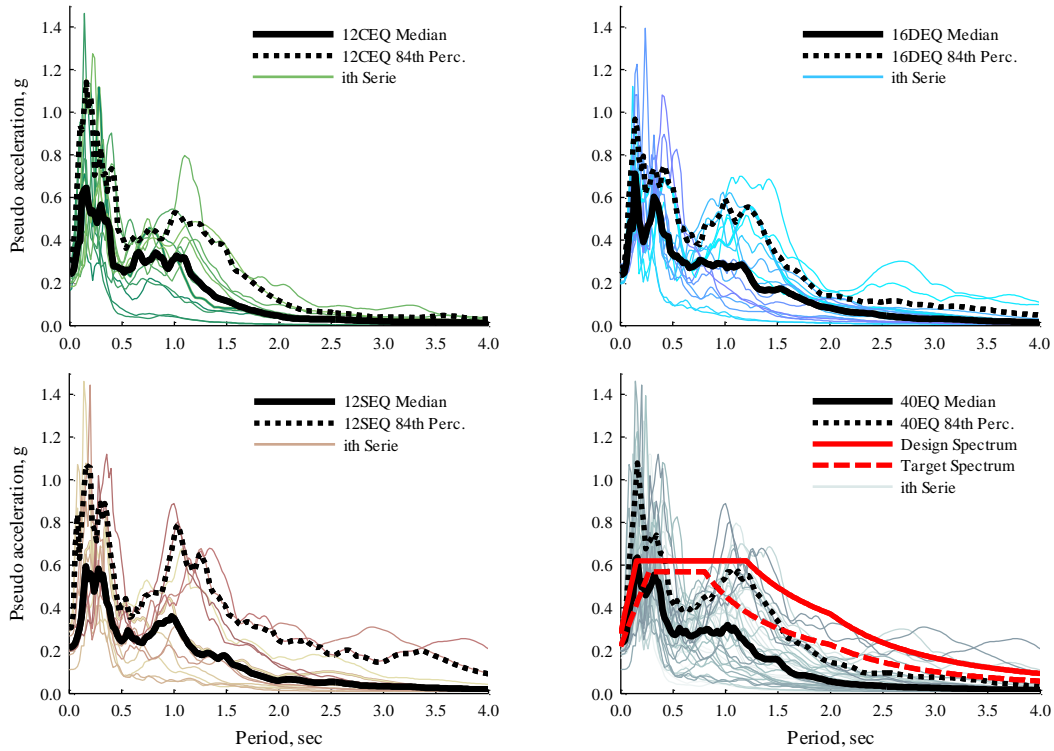


Figure 1. Response spectra ($\zeta = 5\%$): (a) crustal scenario; (b) deep subduction scenario; (c) shallow subduction scenario; (d) complete set of 40 ground motions, design spectrum and minimum target spectrum.

Although it is not shown in this paper, the site response analysis revealed that the soil profile introduces important amplifications and modifications to the ground motions along the entire period range of interest. It is also observed that the pseudo acceleration response spectra for the three hazard scenarios are characterized by two main peaks: one peak at short periods [0 to 0.5 sec] and a second peak at around 1 second which is close to the period of the soil profile (i.e. $T_{soil} = 0.95$ s). For the case of deep and shallow subduction earthquakes it is also important to highlight the site response amplification effects in the long period range [1 to 3 sec].

3. STRUCTURES DESCRIPTION, ANALYSIS AND DESIGN

Two reinforced concrete structures are subjects of research for this study. The first one is a 4 story building (14.4 m of total height) with vertical and lateral-load-resisting-systems comprising of special moment resisting frames and a special I-shaped wall (Figure 2a). The second building has 12 stories (total height of 43.2 m) with vertical and lateral-load-resisting-systems composed by special moment resisting frames, special planar walls and special C-shaped and I-shaped walls (Figure 2b). Both structures have general floor plan dimensions of 32 m in the EW-direction and 21 m in the NS-direction with beam spans ranging from 4.9 to 8.0 m center to center. Given the estimated high seismic hazard, according to NSR-10 the structural systems of the 4-story building (4SB) and the 12-story building (12SB) were classified as “Dual”, both with special detailing of the reinforcement. The assigned response modification factors were: $R_{4SB} = 7.0$ and $R_{12SB} = 8.0$ for the 4SB and 12SB respectively.

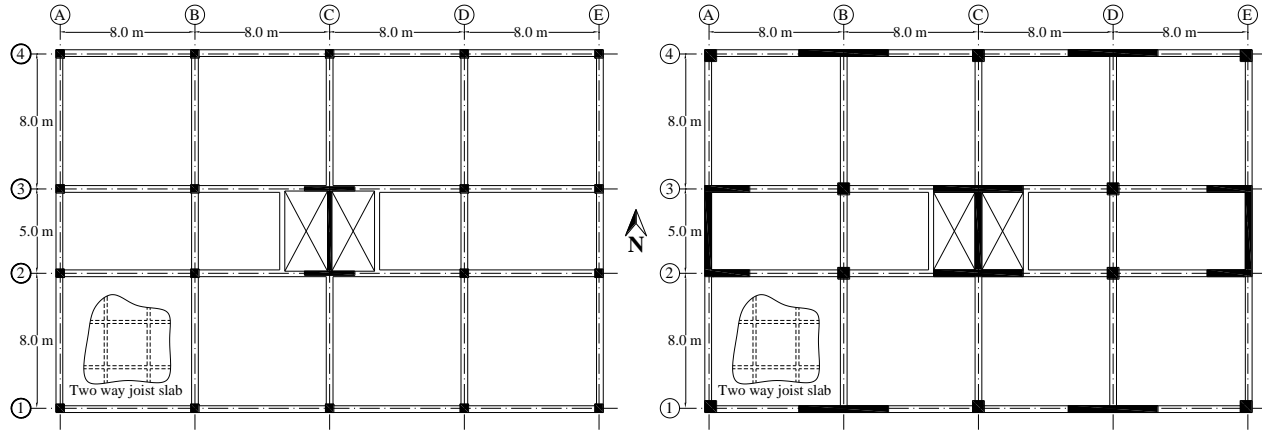


Figure 2. Layout of structural elements of the floor system, columns and structural walls: (a) 4SB, (b) 12SB.

Analyses for combined gravity and lateral seismic loads were done in accordance with NSR-10 and ASCE-7. A three-dimensional, linear structural model of the building was implemented in the computer software ETABS (CSI, 2008). The analyses accounted for degraded stiffness of the structural elements due to seismic loading. The effective inertia of the beams was set to 35% of the gross and those of the columns and walls were set to 70% and 50% respectively. Concrete was assumed normal weight ($\gamma_c = 24 \text{ kN/m}^3$) with nominal strength of 21 and 24 MPa for the 4SB and 24 and 28 MPa for the 12SB. In each building, concrete with the lowest strength was used for the floor systems and higher for the columns and walls. The elastic modulus of the structural elements was computed as $4700\sqrt{f'_c}$ [MPa]. Reinforcing steel was assumed to have a yielding strength of 420 MPa and an elastic modulus of 200,000 MPa.

Rigid diaphragms and masses located at the centre of mass of each floor were used for the linear mathematical models. Modal spectral analyses were performed over the structures to calculate the seismic demand on all structural elements. The design spectrum depicted in Figure 1d was used as the seismic demand. Fundamental periods were $T_{IEW4SB} = 0.96 \text{ s}$, $T_{INS4SB} = 0.58 \text{ s}$ for the EW-direction and NS-direction of the 4SB; for the 12SB the periods were $T_{INS12SB} = 1.65 \text{ s}$ and $T_{IEW12SB} = 1.56 \text{ s}$ for the NS-direction and EW-direction respectively. Design base shears including response modification factor R and scaling to equivalent-lateral-force base shears, were $Vb_{EW4SB} = 2070 \text{ kN}$, $Vb_{NS4SB} = 2090 \text{ kN}$ for the 4SB and $Vb_{NS12SB} = 6530 \text{ kN}$ and $Vb_{EW12SB} = 6830 \text{ kN}$ for the 12SB. Maximum inter-story drift ratios including scaling to equivalent-lateral-force method and cracked sections as described above were 1.76% and 0.82% for EW-direction and NS-direction of the 4SB and 1.8% and 2.0% for EW-direction and NS-direction of the 12SB.

Design of the structural elements (beam, columns and walls) was done in accordance with NSR-10 and ACI-318. The design of two key structural elements (columns and I-shaped walls) of the 4SB and 12SB is summarized in Figures 3 and 4.

For the 4SB, columns were 500 x 500 mm with longitudinal steel ratio (total area of steel to gross area ratio) of $\rho = 1.16\%$ and transverse steel ratio $A_v/b_s = 0.008$ in both directions. Beams were 400 x 600 mm with longitudinal steel ratios (area of tension reinforcement divided by web width and effective depth) ranging from $\rho = 0.33$ to 0.77%. The I-shaped wall (Figure 4a) had the following general dimensions: $b_f = 3,000 \text{ mm}$, $t_f = 250 \text{ mm}$, $d = 4,700 \text{ mm}$ and $t_w = 250 \text{ mm}$. Due to high demand on the wall, boundary elements were provided in the first two stories. The vertical steel ratio of the wall varied from $\rho_l = 0.26\%$ to 0.45% and the horizontal steel ratio was in the range of $\rho_t = 0.26\%$ to 0.53%.

For the 12SB, columns were 1000 x 1000 mm in the first 6 stories and 700 x 700 mm for the upper stories

with longitudinal steel quantities of $\rho = 1.07\%$ and $\rho = 1.16\%$ respectively. Transverse steel quantities varied from $A_v/b_s = 0.0036$ to 0.0064 in both directions. Beams were 400×600 mm with longitudinal steel ratios ranging from $\rho = 0.33$ to 0.68% . The planar walls had dimensions $h_w = 5,330$ mm and $t_w = 400$ mm; the I-shaped walls had (Figure 4b) dimensions $b_f = 5,330$ mm, $t_f = 400$ mm, $d = 4,600$ mm and $t_w = 400$ mm; the C-shaped walls had dimensions $b_f = 2,670$ mm, $t_f = 400$ mm, $d = 4,600$ mm and $t_w = 400$ mm. Due to high demand on the wall, boundary elements were provided in the first half of the height of the wall. The vertical steel ratio of the walls varied from $\rho_l = 0.28\%$ to 0.65% and the horizontal steel ratio was in the range of $\rho_t = 0.28\%$ to 0.50% .

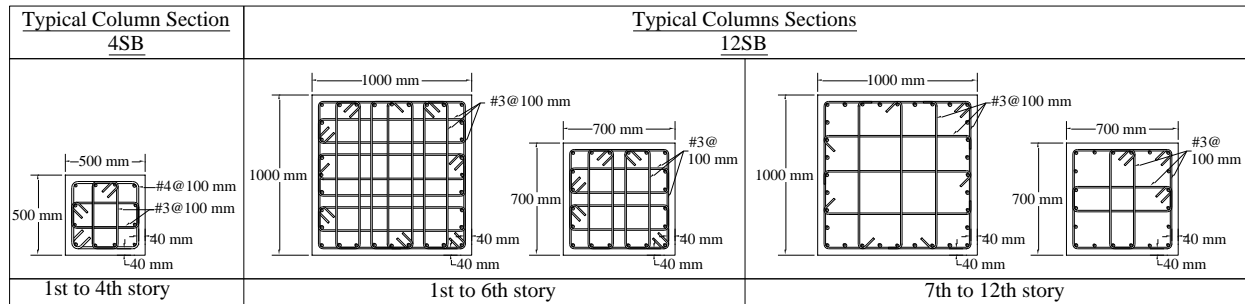


Figure 3. Columns reinforcement detailing

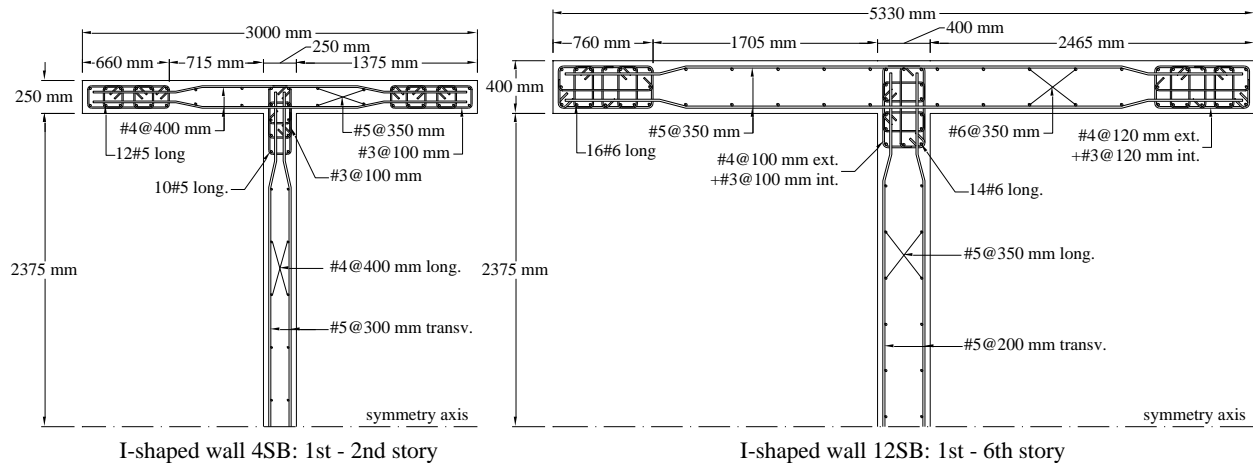


Figure 4. Wall 2C cross section at bottom stories: (a) 4SB, 1st and 2nd story; (b) 12SB, 1st to 6th story.

4. NONLINEAR MODEL FOR SEISMIC PERFORMANCE ASSESSMENT

After designing the buildings, nonlinear mathematical models of the structures were constructed to assess their performance under the scenarios of seismic hazard chosen in Section 2. The software package OpenSees (McKenna et al., 2000) was selected as the nonlinear modelling tool because its nonlinear analysis capabilities allow conducting a large number of simulations and its efficacy has been validated by the research community for many years. Static nonlinear analyses (“pushover”) and dynamic nonlinear analyses were performed over the structures.

Symmetry of the structures allowed for the modelling of half the structural framing in the EW-direction (Figure 5). The previous simplification was done to reduce the amount of time required for each of the 40

simulations. To simulate the large in-plane stiffness of the floors, rigid diaphragm constraints were imposed in each floor of the mathematical model. To represent second-order effects, P-Delta type of geometric transformation was used for the columns while the moderate expected drift demand allowed for the use of linear geometric transformation in the beams.

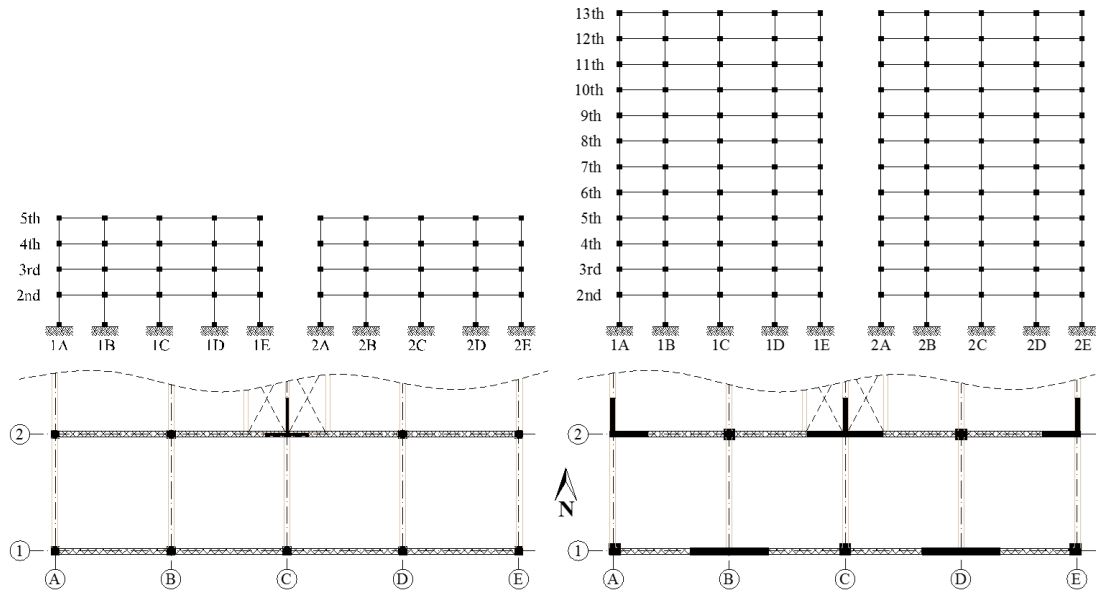


Figure 5. Configuration of the selected frames for the nonlinear analyses: (a) 4SB; (b) 12SB

Nonlinear elements with distributed plasticity and fiber sections at the integration points (Spacone et al., 1996) were used to model all structural elements. The fiber sections allowed for the use of actual uniaxial stress-strain relationships for the different materials in every section. Concrete was modeled as either confined or unconfined (Mander et al., 1988) depending on location within the cross section and its hysteretic behaviour followed the rules by Karsan and Jirsa, 1969. The longitudinal reinforcing steel stress-strain behaviour was assumed to be bilinear with isotropic strain hardening (Filippou et al., 1983). With this approach, the variations of curvature along the elements as well as the effects of axial loads on moment-curvature relations were correctly approximated. Nonlinear shear behaviour of structural elements was not accounted for during the analyses.

For the nonlinear dynamic analyses, mass and stiffness-proportional Rayleigh damping was used to simulate the energy dissipation characteristics of the building that is not accounted for by the nonlinear behaviour of the structural elements. The Rayleigh damping coefficients were established to achieve a damping ratio of $\zeta = 2.5\%$ at periods corresponding to the first and third translational vibration modes of the linear model. Calculated periods for the nonlinear model were $T_{IEW-NL-4SB} = 0.88$ s and $T_{IEW-NL-12SB} = 1.41$ s.

5. RESULTS FROM THE NONLINEAR ANALYSES

5.1 Pushover analyses

Figure 6 shows pushover curves of the planar models (Figure 5) that were developed in the East-West direction. Two lateral load patterns were used to “push” the structures: one proportional to the elastic first mode shape of each building and another one constant along the height of the structures. Lateral loading was terminated when roof drift ratio (displacement of the roof to total height ratio) reached 3.5%. The

pushover curves depict an adequate ductile behaviour of both structures. It is observed that P-Delta effects soften the behavior of the 4SB and 12SB at roof drift ratios of 2.0% and 2.7% approximately. Comparing design base shear demand versus actual capacity of the structure, Figure 6 show global overstrength factors of approximately 2.5 for the 4SB and 2.2 for the 12SB in average. The pushover curves show some evidences of minor degradation due to high compressive demand in the flange of the central walls at roof drift ratios of 0.8% for the 4SB and 1.6% for the 12SB.

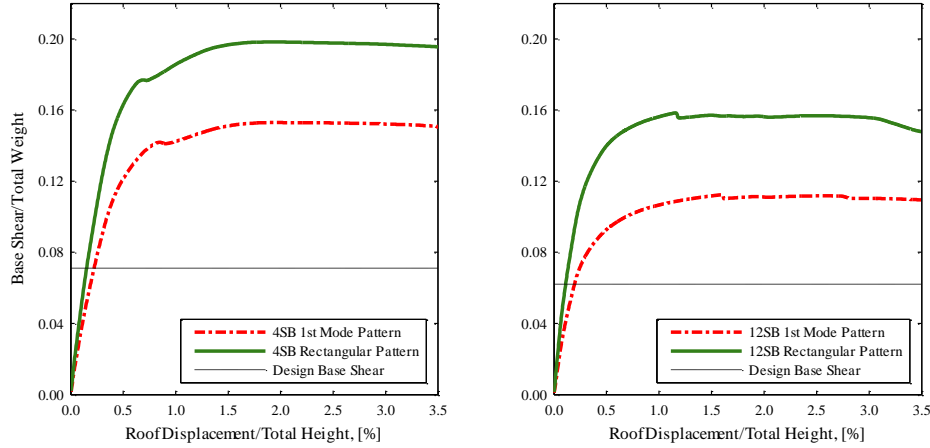


Figure 6. Pushover curves: (a) 4SB, (b) 12SB.

5.2 Nonlinear dynamic analyses

The natural vibration periods of the structures were calculated after each one of the 40 nonlinear dynamic analyses were performed on the mathematical models. Results indicate that the fundamental period of the nonlinear model lengthen an average 30% for the 4SB and 9% for the 12SB (i.e. $T_{1EW-NL-4SB-Final-ave} = 1.15$ s and $T_{1EW-NL-12SB-Final-ave} = 1.54$ s). A stiffness degradation parameter (ψ) was defined according to:

$$\psi = 1 - (T_o/T_f)^2 \quad (1)$$

where T_o is the fundamental period of the structure after gravity loads are applied (i.e. $T_{1EW-NL-4SB} = 0.88$ s and $T_{1EW-NL-12SB} = 1.41$ s) and T_f is the degraded fundamental period of the nonlinear model after each ground motion is applied as uniform excitation at the base. Application of Equation 1 to both structures under the 40 ground motions resulted in average stiffness degradation of $\psi_{4SB-ave} = 37\%$ and $\psi_{12SB-ave} = 14\%$ for the 4SB and 12SB respectively.

Figures 7 and 8 plot inter-story drift ratios and story shears from the code-level elastic analyses and from the nonlinear response history analyses. Values corresponding to median and 84th percentile of the 40 nonlinear dynamic analyses are also shown. Story drifts are conservatively estimated by code level-design forces because of two reasons: i) cracked-sections assumed in the linear analysis underestimate the initial stiffness of the structures under gravity loading alone (e.g. $T_{1-4SB-linear} = 0.95$ s versus $T_{1-4SB-nonlinear} = 0.88$ s and $T_{1-12SB-linear} = 1.56$ s versus $T_{1-12SB-nonlinear} = 1.41$ s), and ii) because the design level spectrum is higher than the median of the 40 earthquakes. It can be observed that the elastic analyses underestimate global story shears by a factor of at least 2.0 for the 4SB and 1.5 for the 12SB with respect to the median responses to the 40 ground motions. Alternative analysis performed on the central wall of the 12SB showed that shear demand calculations including dynamic amplification factors that account for actual flexural strength of the wall (Rejec et al., 2011) and participation of shears from higher modes without reduction by R resulted in better estimations of the design shear demands on the structural element.

Figures 9 and 10 present selected bending moment and shear forces in Wall 2C as obtained from the code-compliant elastic analysis and the nonlinear dynamic analyses for the 4SB and 12SB respectively. The nominal bending moment and shear force capacity is also shown. For the 4SB, bending moment and shear force demand over the central wall are underestimated by the linear elastic analysis for all floors. This result is typical for the columns as well, especially for demands at the base. The depicted wall in Figure 9 has demands above its nominal flexural capacity at the base for the majority of the earthquakes and, maximum bending moment capacity also develops. The median shear demand over the wall of the 4SB is larger than the capacity level at the first and second story. In Figure 10, it is observed that the 12SB showed a similar trend where the elastic analysis underestimate the median demand from the nonlinear analyses.

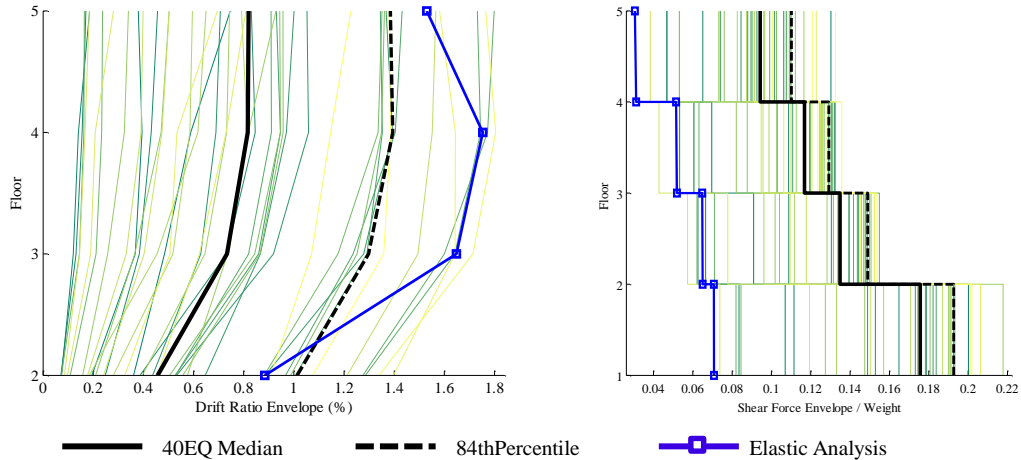


Figure 7. Global structural responses 4 story building (4SB)

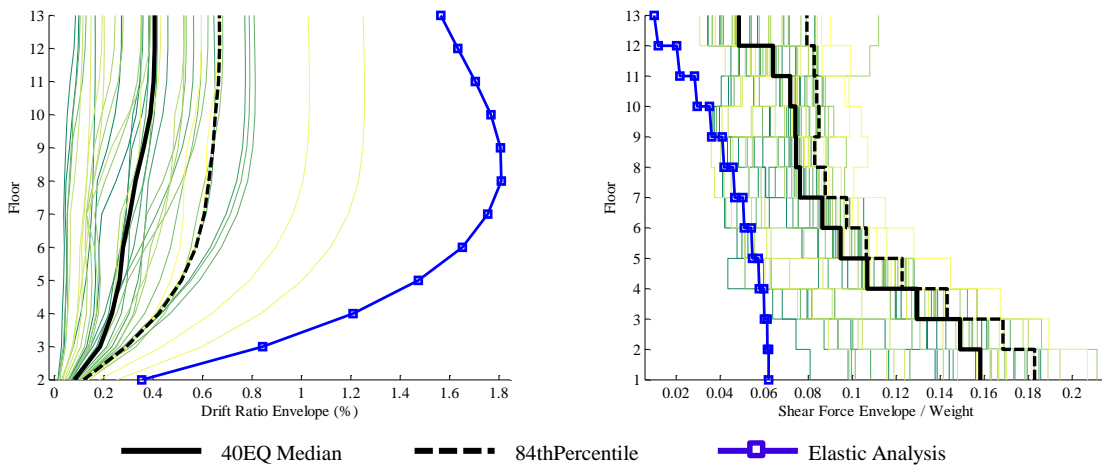


Figure 8. Global structural responses 12 story building (12SB)

Figure 11 shows global structural responses comparison at the median level for the three different scenarios of seismic hazard (data presented are for the 12-story building). The crustal scenario is the less demanding among all three. It is observed that the subduction scenarios demand the structure in an almost identical manner and above the median level of all scenarios combined. Constraints imposed for the horizontal peak ground acceleration range in the selection of the ground motions and filtering exerted by the deep soil column in the site-specific response analysis explain the small variability of the median responses.

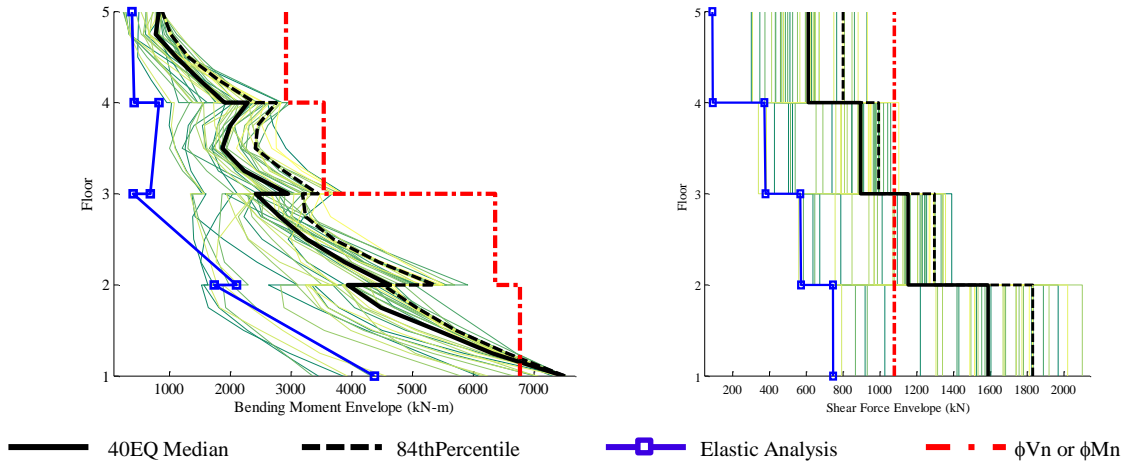


Figure 9. 4SB – Capacity versus demand comparison on Wall 2C: (a) maximum bending moments; (b) maximum shears.

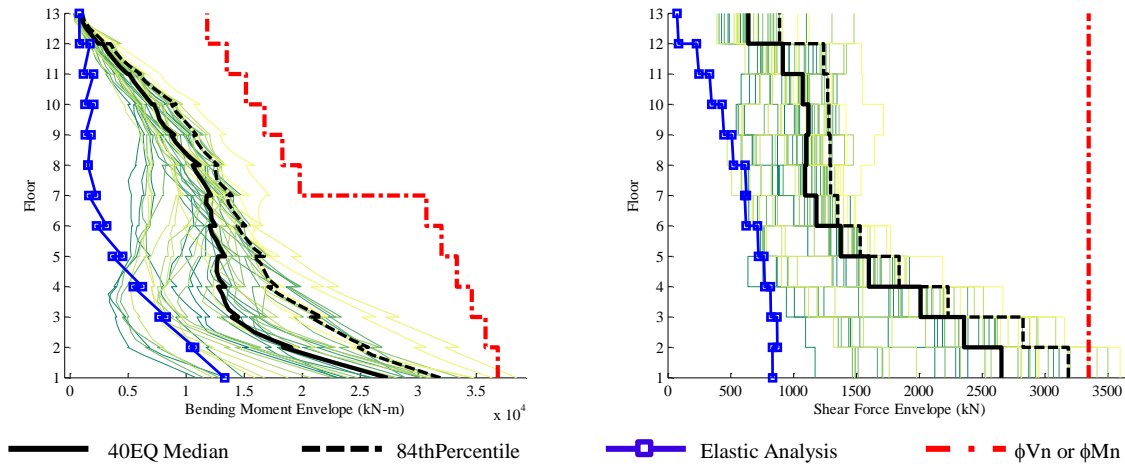


Figure 10. 12SB - Capacity versus demand comparison on Wall 2C: (a) maximum bending moments; (b) maximum shears.

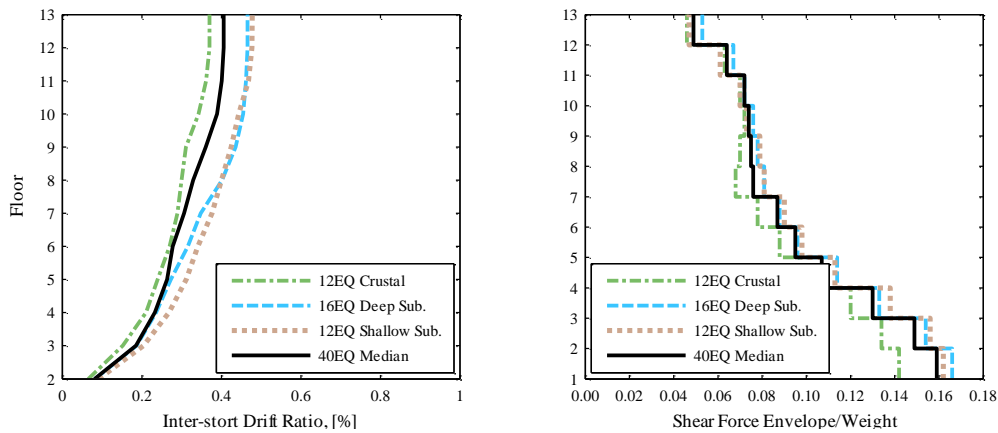


Figure 11. 12SB - Demand comparison of the three hazard scenarios d: (a) inter-story drift ratio; (b) story shear.

6. FINAL COMMENTS

Two structures were designed to comply with current building codes and their performances were assessed via 40 nonlinear response history analyses with ground motions from three probable sources of seismic hazard. Through a site specific response analysis, the frequency content and amplitude of the 40 time series in rock were modified to account for the contribution of the dynamic properties of a column of soft soil. This resulted in a moderate scenario of seismic demand. Structural responses at a global level were gathered from the linear elastic and nonlinear analyses along with response at an element level.

Results show that even though the three scenarios of realistic seismic demand used for the assessment of the buildings were low compared to the seismic demand imposed for design, the shear demands at both the global level and at the element level were underestimated by the design method. Bending moment demands exhibited the same behavior. Of interest is the possibility of brittle failure of the wall of the four-story building, which reached shear demand exceeding capacity in more than 85% of the cases. Similar results were obtained for the twelve-story building. Design shear forces on the walls should include amplification factors to account for actual flexural strength and nonlinear dynamic response.

ACKNOWLEDGEMENT

The authors would like to express their gratitude to Carlos Alvarado from the Colombian Geological Service (INGEOMINAS) for his support in providing valuable information for the site specific response analyses and ground motion selection.

REFERENCES

- ACI Committee 318. (2011). Building Code Requirements for Structural Concrete and Commentary (ACI 318-08), American Concrete Institute, Farmington Hills, USA.
- ASCE. (2006). Minimum Design Loads for Buildings and Other Structures (ASCE/SEI 7-05), American Society of Civil Engineering/ Structural Engineering Institute, Reston, USA.
- CSI. (2008). ETABS – Extended 3D Analysis of Building Systems (Version 9.5.0) [software], Computers and Structures, Inc., Berkeley, USA.
- Filippou, F.C., Popov, E.P. and Bertero, V.V. (1983). Effects of bond deterioration on hysteretic behavior of reinforced concrete joints. Report UCB/EERC-83/19, Earthquake Engineering Research Center, University of California, Berkeley, USA.
- INGEOMINAS. (2005). Microzonificación Sísmica de la Ciudad de Santiago de Cali, Bogotá, Colombia.
- Karsan, I.D., and Jirsa, J.O., (1969). Behavior of concrete under compressive loadings. *Journal of Structural Division*, **95:12**, 2543-2563, ASCE.
- Mander, J. B., Priestley, M. J. N., and Park, R. (1988). Theoretical stress-strain model for confined concrete. *Journal of Structural Engineering*, **114:8**, 1804-1825, ASCE.
- McKenna, F., Fenves, G. L., Scott, M. H., and Jeremic, B. (2000). Open System for Earthquake Engineering Simulation (OpenSees) [software]. Pacic Earthquake Engineering Research Center, University of California, Berkeley, USA.
- NSR-10. (2010). Reglamento Colombiano de Construcción Sismo Resistente (NSR-10), Asociación Colombiana de Ingeniería Sísmica (AIS), Bogotá, Colombia.
- Ordoñez, G.A. (2000). SHAKE 2000 User's Manual, (Internet). Available from <<http://www.geomotions.com/Download/SHAKE2000Manual.pdf>> (Accessed 24 April, 2012).
- Rejec, K., Isaković, T. and Fischinger, M. (2011). Seismic shear force magnification in RC cantilever structural walls, designed according to Eurocode 8. *Bulletin of Earthquake Engineering*, **10:2**, 567-586, Springer.
- Spacone, E., Filippou, F. C. and Taucer, F. F. (1996). Fibre beam-column model for non-linear analysis of R/C frame: Part I. Formulation. *Earthquake Engineering and Structural Dynamics*, **25:7**, 711-725, John Wiley and Sons, Ltd.